

*Journal of Organometallic Chemistry*, 214 (1981) 93–105  
Elsevier Sequoia S.A., Lausanne — Printed in The Netherlands

## [3]FERROCENOPHANE BRIDGE REVERSAL BARRIERS

### II \*. CARBON, OXYGEN AND SULPHUR BRIDGING ATOMS

EDWARD W. ABEL, MARTIN BOOTH, CAROL A. BROWN, KEITH G. ORRELL and  
RODNEY L. WOODFORD

*Department of Chemistry, The University, Exeter EX4 4QD (Great Britain)*

(Received December 9th, 1980)

#### Summary

Variable temperature NMR studies have shown that, at temperatures below  $-100^{\circ}\text{C}$ , the bridge reversal process in [3]ferrocenophane is slow on the NMR time scale and studies have yielded an energy barrier of  $40.4\text{ kJ mol}^{-1}$  for this process, a value lower than that for ring reversal in cyclohexane. Other [3]ferrocenophanes with six-membered ring analogues have also been studied and the data obtained have allowed interesting comparisons between the bridge and ring reversal processes to be made. A number of torsional barriers about carbon–chalcogen and chalcogen–chalcogen bonds have also been calculated.

---

#### Introduction

We have recently investigated a variety of fluxional phenomena including six-membered heterocyclic ring reversal [1,2] and [3]ferrocenophane bridge reversal [3,4]. In our previous paper [4] we showed how the application of dynamic NMR techniques to [3]ferrocenophanes containing chalcogen bridging atoms led to particularly accurate energy barriers for the bridge reversal process. The values obtained enabled relative torsional barriers about bridge bonds to be calculated and, in the case of  $\text{Cp}_2\text{FeS}_3$ , analogies with the ring reversal process of the six-membered ring  $(\overline{\text{CH}_2})_3\text{S}_3$  were made. In order to gain further insight into the factors governing such bridge reversal barriers we have extended these studies to include other [3]ferrocenophanes with six-membered ring analogues, namely the compounds  $\text{Cp}_2\text{FeX}_2\text{Y}$  ( $\text{X} = \text{CH}_2$ ;  $\text{Y} = \text{CH}_2, \text{O}$  or  $\text{S}$ ;  $\text{X} = \text{S}$ ;  $\text{Y} = \text{CH}_2$  or  $\text{CMe}_2$ ).

---

\* For part I see ref. 4.

## Experimental

All the [3]ferrocenophanes were examined in  $\text{CD}_2\text{Cl}_2/\text{CS}_2$  mixed solvent solutions. Variable temperature NMR spectra were recorded between  $-120^\circ\text{C}$  and ambient temperature at  $5-10^\circ\text{C}$  intervals. A JEOL PS/PFT-100 spectrometer was used to record the 25 MHz  $^{13}\text{C}$  and 100 MHz  $^1\text{H}$  spectra and a Perkin-Elmer R34 spectrometer at P.C.M.U. Harwell was used for the 220 MHz  $^1\text{H}$  spectra. A JES-VT-3 unit was used to control the probe temperatures which were measured, using a Comark digital thermometer type 5000 attached to a Cu/Cu-Ni thermocouple adapted for use in the NMR probe, to an accuracy of at least  $\pm 1^\circ\text{C}$ .

All the compounds studied have been synthesised previously. [3]Ferrocenophane  $[\text{Cp}_2\text{Fe}(\text{CH}_2)_2\text{CH}_2]$  was prepared in a novel way by treatment of 1,1'-dilithioferrocene with 1,3-dibromopropane to yield [3]ferrocenophane directly; however yields using this method were low, and on balance we feel that the original method of Rosenblum et al. [5] is to be preferred. 2-Oxa[3]ferrocenophane  $[\text{Cp}_2\text{Fe}(\text{CH}_2)_2\text{O}]$  was prepared in good yields using the method of Yamakawa and Hisatome [6]. The sample of 2-thia[3]ferrocenophane  $[\text{Cp}_2\text{Fe}(\text{CH}_2)_2\text{S}]$  was donated by Drs. A.G. Osborne (of this Department) and R.H. Whiteley. The compounds 1,3-dithia[3]ferrocenophane  $[\text{Cp}_2\text{FeS}_2\text{CH}_2]$  and 1,3-dithia-2,2-dimethyl[3]ferrocenophane  $[\text{Cp}_2\text{FeS}_2\text{CMe}_2]$  were prepared from  $\text{Cp}_2\text{FeS}_3$  using the method of Davison and Smart [7].

## Results

Bridge reversal barriers were computed in the usual way from analyses of variable temperature spectra [8,9]. In contrast to the chalcogen bridged [3]ferrocenophanes [4] the spectra of the compounds studied here all exhibited distinctive features and will be described individually.



The analogy between [3]ferrocenophane and cyclohexane (Fig. 1) was first

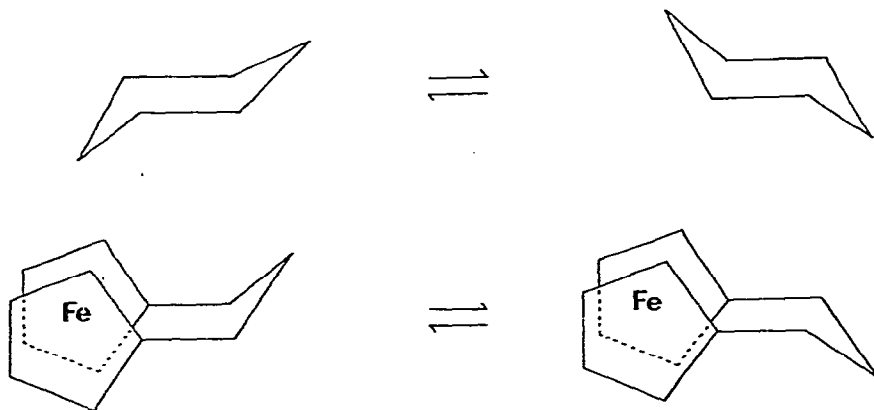


Fig. 1. The analogy between the bridge and ring reversal processes.

recognised by Rosenblum et al. [5] who interpreted the relatively simple room temperature spectrum of  $\text{Cp}_2\text{Fe}(\text{CH}_2)_2\text{CH}_2$  as arising from a situation where bridge reversal was rapid. Later work [10] failed to "freeze out" this motion at  $-55^\circ\text{C}$ , the low temperature limit of the solvent ( $\text{CDCl}_3$ ) used. By choosing a more suitable solvent system ( $\text{CD}_2\text{Cl}_2/\text{CS}_2$ ) we have been able to obtain  $^1\text{H}$  spectra of  $\text{Cp}_2\text{Fe}(\text{CH}_2)_2\text{CH}_2$  at temperatures between  $-53^\circ\text{C}$  and  $-120^\circ\text{C}$ . The methylene region of these spectra is illustrated in Fig. 2.

Assuming rapid bridge reversal to be occurring at  $-50^\circ\text{C}$  and above, the expected  $^1\text{H}$  spectra in this temperature range should consist of two distorted triplets, arising from an  $\text{AA}'\text{BB}'$  spin system for the Cp protons, and two complex multiplets in the ratio 2/1 corresponding to the two types of methylene protons. However, as a result of accidental equality of certain chemical shifts, only two bands were observed at room temperature. Upon cooling the sample to  $-100^\circ\text{C}$ , both regions of the spectra became more complex but underwent no further significant changes below this temperature. To facilitate the interpretation and analysis of these spectra a 220 MHz spectrum was recorded at  $-100^\circ\text{C}$ . This is illustrated in Fig. 3 together with its computer simulation.

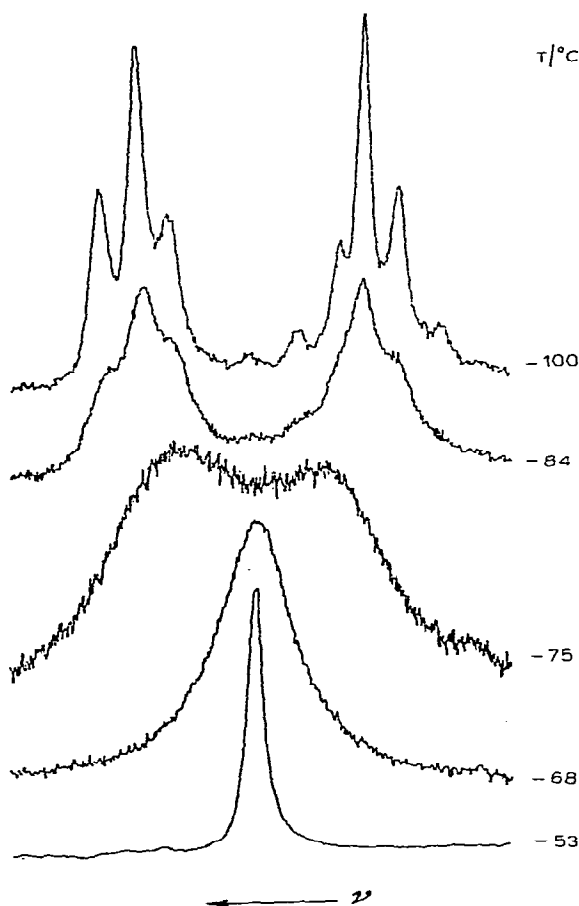


Fig. 2. Variable temperature 100 MHz  $^1\text{H}$  spectra of  $\text{Cp}_2\text{Fe}(\text{CH}_2)_2\text{CH}_2$  (methylene region).

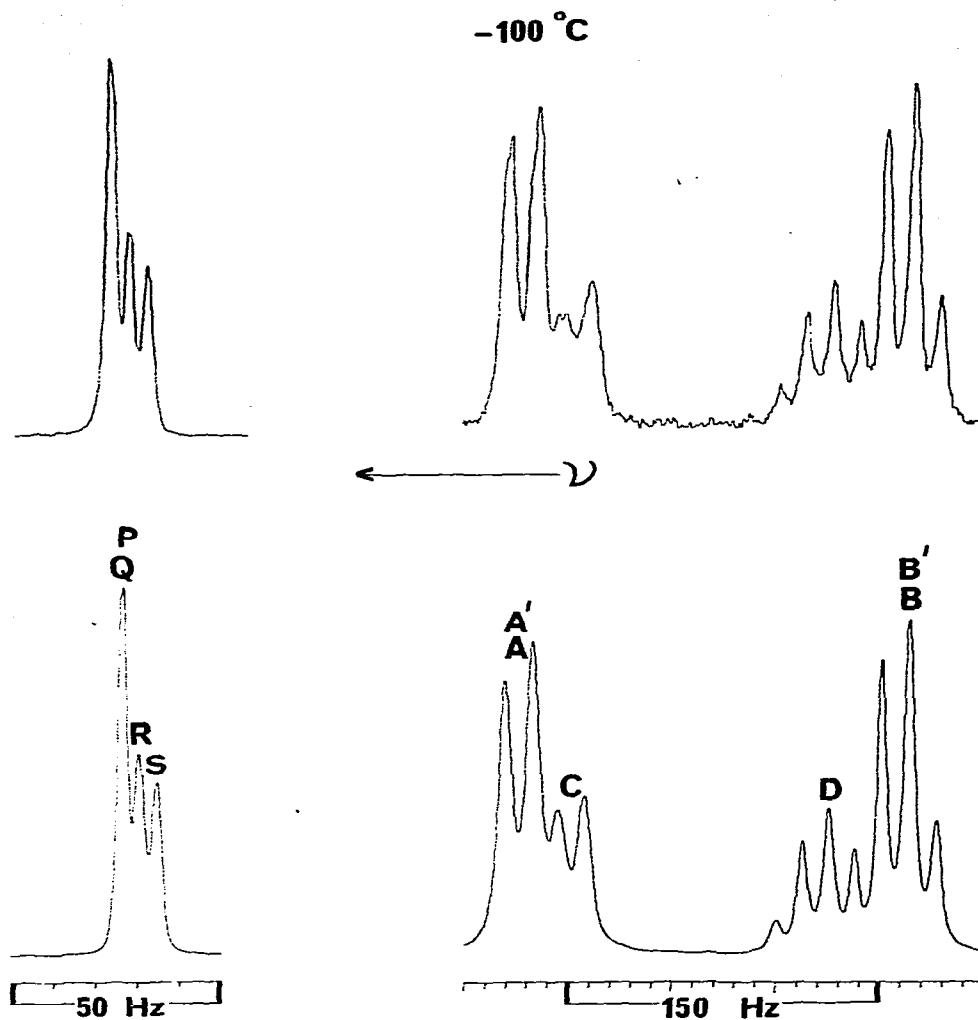


Fig. 3. 220 MHz spectrum of  $\text{Cp}_2\text{Fe}(\text{CH}_2)_2\text{CH}_2$  and its computer simulation.

The computer simulation of the Cp region was readily performed by treating the spectrum as a 4 spin problem (Fig. 4), as described previously [4]. This gave the chemical shift and coupling constant data for Cp protons in Tables 1 and 2 which show no unusual features [4,11]. Unfortunately attempts to use the changes in the Cp spectral region to calculate the bridge reversal barrier were unsuccessful owing to the small chemical shift differences involved. Our attention was therefore directed towards the interpretation of the methylene region.

The "static" spectrum of this region at  $-100^\circ\text{C}$  (Fig. 3) was treated as an  $\text{AA}'\text{BB}'\text{CD}$  spin system (Fig. 4). The chemical shift values obtained at 220 MHz could be successfully reduced to fit the 100 MHz spectra without error, the values being given in Table 1. The values of the geminal and vicinal couplings were found to be  $J_{\text{AB}} = J_{\text{A}'\text{B}'} = -14.0$  Hz;  $J_{\text{AC}} = J_{\text{A}'\text{C}} = 2.0$  Hz;  $J_{\text{AB}} = J_{\text{A}'\text{D}} = 2.0$  Hz;

TABLE 1  
CHEMICAL SHIFTS AND THEIR TEMPERATURE-VARIABLE COEFFICIENTS FOR ALL PROTONS INVOLVED IN LINE SHAPE ANALYSIS<sup>a</sup>

Compound	Solvent	Reference	$\nu_P$ (Hz)		$\nu_Q$ (Hz)		$\nu_R$ (Hz)		$\nu_S$ (Hz)	
			a	b	a	b	a	b	a	b
<i>Cyclopentadienyl protons</i>										
$Cp_2Fe(CH_2)_2CH_2$	$CD_2Cl_2/CS_2$	TMS	393.4	—	393.4	—	388.1	—	383.5	—
$Cp_2FeS_2CH_2$	$CD_2Cl_2/CS_2$	TMS	437.2	-0.031	433.6	-0.031	429.4	-0.031	376.2	-0.048
$Cp_2FeS_2CMe_2$	$CD_2Cl_2/CS_2$	TMS	427.6	-0.037	436.8	-0.037	431.8	-0.037	379.8	-0.037
Compound	Solvent	Reference	$\nu_{A(A')}$ (Hz)		$\nu_{B(B')}$ (Hz)		$\nu_C$ (Hz)		$\nu_D$ (Hz)	
			a	b	a	b	a	b	a	b
<i>Bridge protons</i>										
$Cp_2Fe(CH_2)_2CH_2$	$CD_2Cl_2/CS_2$	TMS	234.1	—	149.5	—	222.5	—	167.3	—
$Cp_2FeS_2CH_2$	$CD_2Cl_2/CS_2$	TMS	—	—	—	—	430.8	-0.088	397.0	0.033
$Cp_2FeS_2CMe_2$	$CD_2Cl_2/CS_2$	TMS	—	—	—	—	197.3	-0.039	177.0	0.000
$Cp_2Fe(CH_2)_2O$	$CD_2Cl_2/CS_2$	TMS	440.9	-0.025	318.4	-0.025	—	—	—	—
$Cp_2Fe(CH_2)_2S$	$CD_2Cl_2/CS_2$	TMS	321.8	0.000	275.3	0.000	—	—	—	—

<sup>a</sup> Chemical shift ( $\nu_i$ ) from TMS (in Hz) at temperature  $\theta_c$  (°C) is given by the expression  $\nu_i$  (Hz) =  $a + b(\theta_c/^\circ C)$ .

TABLE 2  
SPIN-SPIN COUPLING CONSTANTS (Hz) AND TRANSVERSE RELAXATION TIMES (s)<sup>a</sup> FOR ALL PROTONS INVOLVED IN LINE SHAPE ANALYSIS

Compound	Cyclopentadienyl protons						Bridge protons			$T_2^*$
	J <sub>PQ</sub>	J <sub>PR</sub>	J <sub>PS</sub>	J <sub>QR</sub>	J <sub>QS</sub>	J <sub>RS</sub>	J <sub>AB</sub>	J <sub>CD</sub>		
$Cp_2Fe(CH_2)_2CH_2$	1.25	2.50	1.25	2.50	2.50	1.25	see text	—	—	0.265-0.636
$Cp_2FeS_2CH_2$	1.25	2.50	1.25	2.50	2.50	1.25	—	-14.26	0.0	0.152-0.606
$Cp_2FeS_2CMe_2$	1.25	2.50	1.25	2.50	2.50	1.25	—	—	—	0.122
$Cp_2Fe(CH_2)_2O$	—	—	—	—	—	—	-13.04	—	—	0.121-0.195
$Cp_2Fe(CH_2)_2S$	—	—	—	—	—	—	-14.95	—	—	—

<sup>a</sup>  $T_2^*$  determined from  $\Delta\nu_{1/2} = (\pi T_2^*)^{-1}$ , where  $\Delta\nu_{1/2}$  = natural line width at half-height; see text for further details.

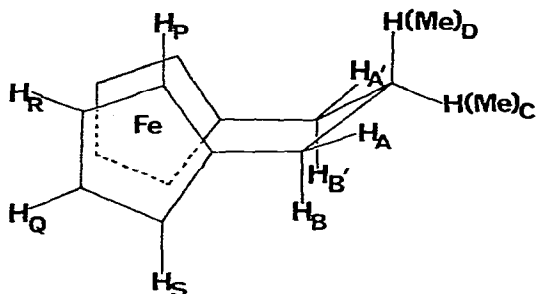


Fig. 4. Static conformation of [3]ferrocenophane showing proton assignments.

$J_{BC} = J_{B'C} = 2.0$  Hz;  $J_{BD} = J_{B'D} = 13.0$  Hz;  $J_{CD} = -13.0$  Hz. The long range  $^4J(\text{HH})$  couplings could not be resolved and were accounted for by using a large value (5 Hz) for the natural line width [12].

The dynamic spin problem for the methylene region undergoing bridge reversal is  $AA'BB'CD \rightleftharpoons B'BA'ADC$  which is too complex for the DNMR computer program. However, we have recently shown that such spin systems can be reduced without significant error to exchanging ABCD systems providing that only the higher frequency AB portion is fitted [12]. Unfortunately in this case such a reduction is impossible because the CD region of the spectra is situated between the A and B regions.

Thus in order to compute the bridge reversal energy we were forced to study the  $^{13}\text{C}$  spectrum of  $\text{Cp}_2\text{Fe}(\text{CH}_2)_2\text{CH}_2$ , a difficult procedure owing to the poor solubility of the compound at low temperatures. At  $-100^\circ\text{C}$  the 25 MHz  $^{13}\text{C}$  spectra of [3]ferrocenophane gave the expected single line for the quaternary Cp carbon ( $\delta$  85.88 ppm), four signals for the methine Cp carbons ( $\delta$  72.08, 69.82, 68.30 and 67.81 ppm) and two signals for the methylene carbons in the intensity ratio 2 ( $\delta$  24.54 ppm)/1 ( $\delta$  35.58 ppm). Upon raising the temperature to ambient, the outer and inner pairs of methine Cp carbon signals broadened and coalesced to give two averaged signals. The spectra at  $-67^\circ\text{C}$  and  $-79^\circ\text{C}$  were simulated as a mutually exchanging 4-spin problem giving values for the rate of bridge reversal at these two temperatures. These data were then utilised to give the value of  $\Delta G^\ddagger(T)$  for  $\text{Cp}_2\text{Fe}(\text{CH}_2)_2\text{CH}_2$  in Table 3.

TABLE 3

COMPARISON OF  $\Delta G^\ddagger(T_c)$  FOR BRIDGE REVERSAL AND RING REVERSAL PROCESSES

Bridge reversal		Ring reversal				
Compound	$\Delta G^\ddagger(T_c)$ (kJ mol $^{-1}$ )	Compound	$T_c$ (K)	$\Delta G^\ddagger(T_c)$ (kJ mol $^{-1}$ )	Ref.	$\Delta\Delta G^\ddagger(T_c)$ (kJ mol $^{-1}$ )
$\text{Cp}_2\text{FeS}_2\text{S}$	80.1	$(\text{CH}_2)_3\text{S}_2\text{S}$	265	55.4	17	+24.7
$\text{Cp}_2\text{FeS}_2\text{CH}_2$	47.2	$(\text{CH}_2)_3\text{S}_2\text{CH}_2$	203	43.5	18	+3.7
$\text{Cp}_2\text{FeS}_2\text{CMe}_2$	42.8	$(\text{CH}_2)_3\text{S}_2\text{CMe}_2$	203	42.3	18	+0.5
$\text{Cp}_2\text{Fe}(\text{CH}_2)_2\text{CH}_2$	40.4	$(\text{CH}_2)_3(\text{CH}_2)_2\text{CH}_2$	206	42.7	19	-2.3
$\text{Cp}_2\text{Fe}(\text{CH}_2)_2\text{O}$	39.7	$(\text{CH}_2)_3(\text{CH}_2)_2\text{O}$	212	43.1	20	-3.4
$\text{Cp}_2\text{Fe}(\text{CH}_2)_2\text{S}$	34.6	$(\text{CH}_2)_3(\text{CH}_2)_2\text{S}$	192	39.5	20	-4.9

TABLE 4  
ARRHENIUS AND ACTIVATION PARAMETERS FOR [3]FERROCENOPHANE BRIDGE REVERSAL

Compound <sup>a</sup>	Solvent	$E_a$ (kJ mol <sup>-1</sup> )	$\log_{10} A$	$\Delta H^\ddagger$ (kJ mol <sup>-1</sup> )	$\Delta S^\ddagger$ (J K <sup>-1</sup> mol <sup>-1</sup> )	$\Delta G^\ddagger$ <sup>b</sup> (kJ mol <sup>-1</sup> )
<u>Cp<sub>2</sub>FeS<sub>2</sub>CH<sub>2</sub></u>	CD <sub>2</sub> Cl <sub>2</sub> /CS <sub>2</sub>	47.60 ± 0.80	12.73 ± 0.18	45.68 ± 0.80	-7.45 ± 3.45	47.90 ± 0.23
Cp <sub>2</sub> FeS <sub>2</sub> CMe <sub>2</sub>	CD <sub>2</sub> Cl <sub>2</sub> /CS <sub>2</sub>	43.39 ± 1.41	12.55 ± 0.35	40.64 ± 1.39	-10.10 ± 6.59	43.65 ± 0.57
<u>Cp<sub>2</sub>FeS<sub>2</sub>CMe<sub>2</sub></u>	CD <sub>2</sub> Cl <sub>2</sub> /CS <sub>2</sub>	45.26 ± 0.92	13.12 ± 0.23	43.51 ± 0.96	3.42 ± 4.35	42.49 ± 0.34
Cp <sub>2</sub> Fe(CH <sub>2</sub> ) <sub>2</sub> O	CD <sub>2</sub> Cl <sub>2</sub> /CS <sub>2</sub>	41.42 ± 1.53	13.07 ± 0.43	39.80 ± 1.52	0.50 ± 7.76	39.65 ± 0.79
<u>Cp<sub>2</sub>Fe(CH<sub>2</sub>)<sub>2</sub>S</u>	CD <sub>2</sub> Cl <sub>2</sub> /CS <sub>2</sub>	35.79 ± 0.81	12.93 ± 0.81	34.37 ± 0.81	-1.15 ± 4.76	34.71 ± 0.61

<sup>a</sup> The underlined portion of the molecule indicates the region of the spectrum used for line shape fitting. <sup>b</sup> Calculated for  $T = 298.15$  K.

$\text{Cp}_2\text{Fe}(\text{CH}_2)_2\text{O}$ 

The  $^1\text{H}$  NMR room temperature spectrum of  $\text{Cp}_2\text{Fe}(\text{CH}_2)_2\text{O}$  in  $\text{CD}_2\text{Cl}_2/\text{CS}_2$  consisted of two distorted triplets for the Cp region and a single peak for the methylene protons. Cooling the sample to  $-100^\circ\text{C}$  resulted in spectral changes consistent with the slowing down of bridge reversal. The Cp region gave four complex signals with relatively small internal chemical shifts and the methylene signal split to give a widely spaced AB quartet pattern. In view of this large chemical shift difference it was decided to compute the bridge reversal energy by simulation of this region of the spectrum.

The spin problem is strictly  $\text{AA}'\text{BB}' \rightleftharpoons \text{B}'\text{BA}'\text{A}$ ; however the long range couplings could not be resolved, and were incorporated into the natural line width

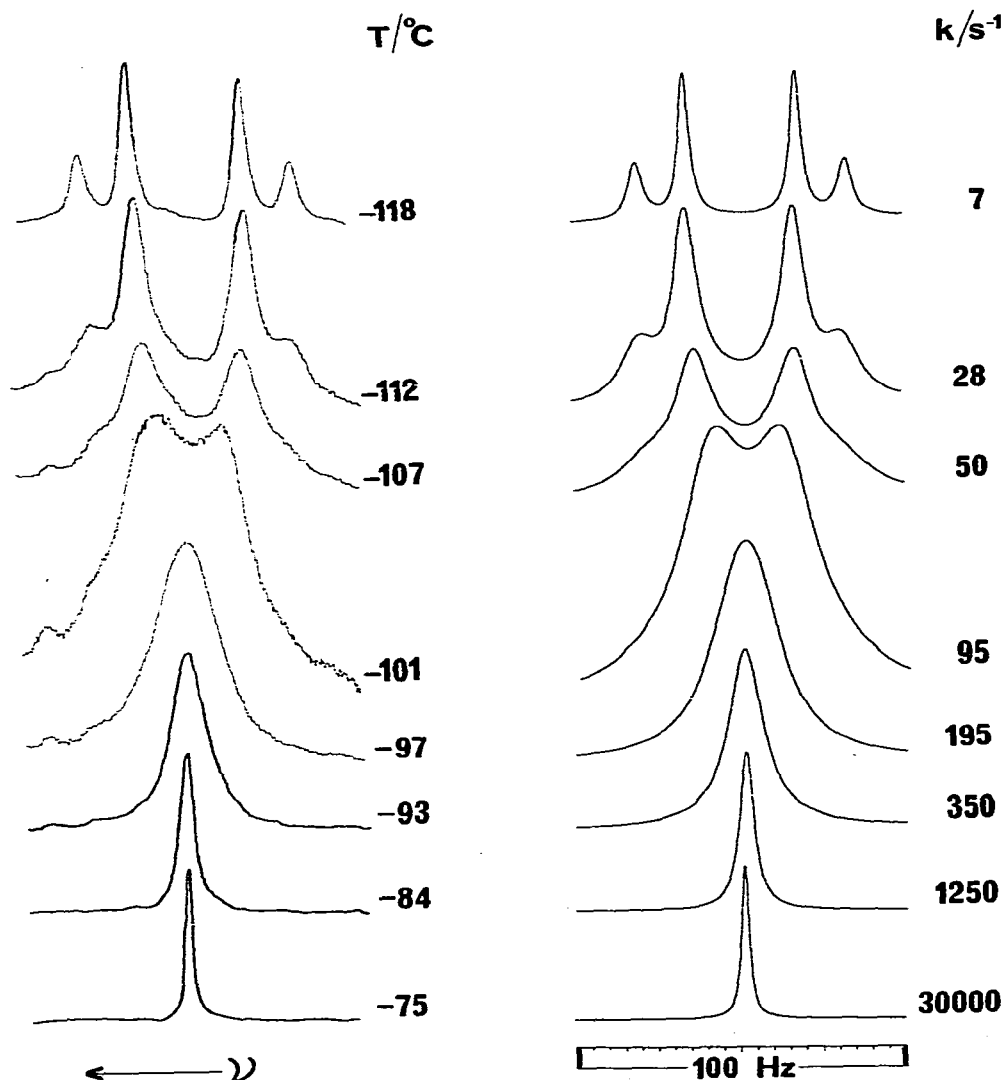


Fig. 5. Experimental and computer synthesised spectra of  $\text{Cp}_2\text{Fe}(\text{CH}_2)_2\text{S}$ .



giving a readily handled  $AB \rightleftharpoons BA$  spin problem. The spectral parameters used in this calculation are listed in Tables 1 and 2. Variable temperature spectra were fitted between  $-110^\circ\text{C}$  and  $-50^\circ\text{C}$  producing bridge reversal energy data listed in Table 4.

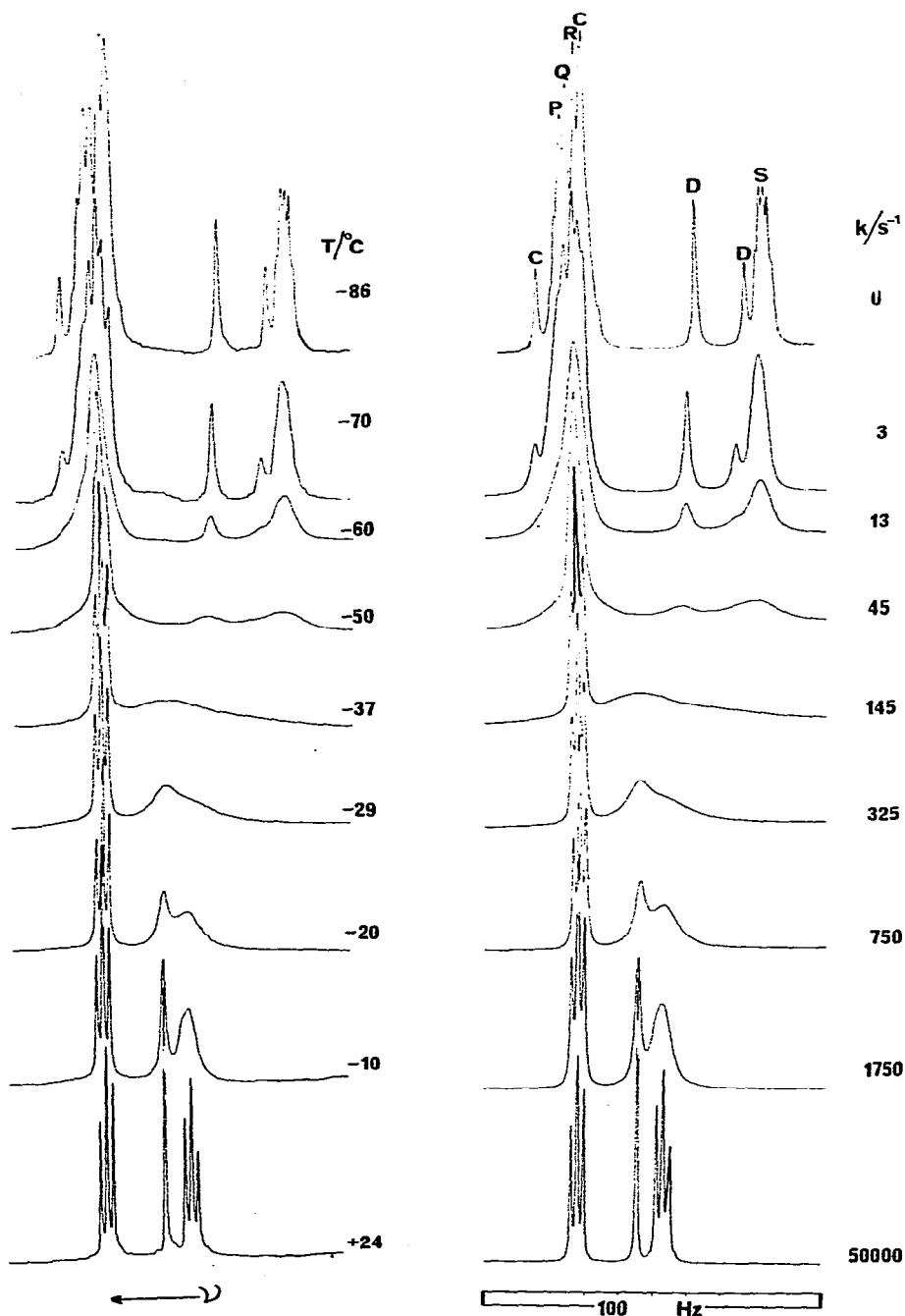


Fig. 6. Experimental and computer synthesised spectra of  $\text{Cp}_2\text{FeS}_2\text{CH}_2$ .

*Cp<sub>2</sub>Fe(CH<sub>2</sub>)<sub>2</sub>S*

The variable temperature <sup>1</sup>H NMR spectra of Cp<sub>2</sub>Fe(CH<sub>2</sub>)<sub>2</sub>S were very similar to those of Cp<sub>2</sub>Fe(CH<sub>2</sub>)<sub>2</sub>O discussed above. However the freezing of the bridge reversal process occurs at a somewhat lower temperature and even at -118°C, the low temperature limit of the solvent used, the spectra were still influenced by the rate process to a small extent. The methylene region, simulated as an AB ⇌ BA spin problem, was again used to calculate the energy for the bridge reversal process. The relevant data are listed in Tables 1 and 2 and a set of spectra together with their simulations are shown in Figure 5. It should be noted that because the rate process is still not slow on the NMR time scale at -118°C the natural line widths in the absence of exchange could not be measured directly and were deduced from the linewidths of the TMS signal. The Arrhenius and activation parameters are listed in Table 4.

*Cp<sub>2</sub>FeS<sub>2</sub>CH<sub>2</sub>*

The spectra of Cp<sub>2</sub>FeS<sub>2</sub>CH<sub>2</sub> were different from those of Cp<sub>2</sub>Fe(CH<sub>2</sub>)<sub>2</sub>S in that the presence of an additional sulphur atom causes the chemical shifts of the methylene protons to overlap with the Cp signals, Fig. 6. This necessitated the analysis of the spectra as two overlapping spin systems CD ⇌ DC and PQRS ⇌ SRQP. The assignments of the six proton signals are illustrated in Fig. 6 and the spectral parameters listed in Tables 1 and 2. The same rate constants were used for fitting both the Cp and CH<sub>2</sub> regions and a set of fits are illustrated in Fig. 6. The energy data are listed in Table 4.

*Cp<sub>2</sub>FeS<sub>2</sub>CMe<sub>2</sub>*

The spectra of Cp<sub>2</sub>FeS<sub>2</sub>CMe<sub>2</sub> were somewhat easier to analyse than those of Cp<sub>2</sub>FeS<sub>2</sub>CH<sub>2</sub> because there was no problem of overlapping signals. However difficulty was experienced in simulating the Cp region, and a satisfactory solution was only possible by the unusual assignment of the protons P and S, adjacent to the S<sub>2</sub>CMe<sub>2</sub> bridge, to the two lowest frequency regions. In all previous cases [4] these protons gave rise to the highest and lowest frequency signals, respectively. As a check on the consistency of our line shape analyses the Cp and methyl regions were independently simulated between -92 and -35°C as PQRS ⇌ SRQP and AX ⇌ XA spin problems, respectively. The spectral parameters are listed in Tables 1 and 2, and the Arrhenius and activation parameters for the two fitting methods are given in Table 4.

**Discussion***Spectral parameters*

The values of the coupling constants for the CH<sub>2</sub> bridge protons at -100°C given in the text are an interesting pointer to the structure of [3]ferrocenophane. X-ray analyses of [3]ferrocenophanes [13,14] have consistently shown a half chair conformation of the bridge, Fig. 4. Such a conformation for Cp<sub>2</sub>Fe-(CH<sub>2</sub>)<sub>2</sub>CH<sub>2</sub> in solution is confirmed by the vicinal couplings, the values of which are similar to those recently determined for cyclohexane-1,1,2,2,3,3,4,4-*d*<sub>8</sub> [15].

The only unusual feature of the Cp data (Tables 1 and 2) is the assignments

of the Cp protons adjacent to the bridge in  $\text{Cp}_2\text{FeS}_2\text{CMe}_2$  to the lowest frequency signals. This must reflect additional shielding of proton P by the  $\text{CMe}_2$  group as compared to that of the  $\text{CH}_2$  group.

The AB quartet patterns for the compounds  $\text{Cp}_2\text{Fe}(\text{CH}_2)_2\text{X}$  ( $\text{X} = \text{O}$  or  $\text{S}$ ) show a greater chemical shift difference for the case when  $\text{X} = \text{O}$  reflecting the greater proximity of the oxygen lone pairs to the  $\text{CH}_2$  groups. The assignments of individual methylene protons are not obvious except in the case of  $\text{Cp}_2\text{Fe}(\text{CH}_2)_2\text{CH}_2$  where the axial protons of both methylene groups, B and D (Fig. 4), are confidently assigned to the lowest frequency signals (Table 1). These assignments are based on the magnitudes of the vicinal couplings the values of which are similar to those found for cyclohexane derivatives [15].

### Torsional barriers

In our previous paper [4] we have described a method for calculating relative torsional barriers ( $\Delta V$ ) about single bonds containing Group VI atoms. In a similar way the values of  $\Delta G^\ddagger$ , listed in Table 4, can be used to calculate a num-

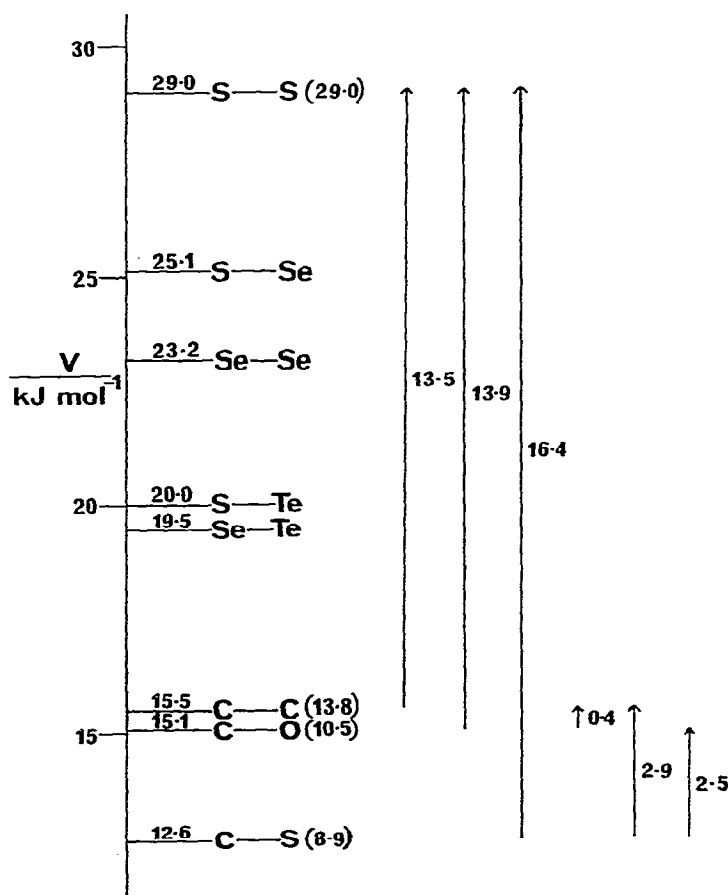


Fig. 7. Absolute and relative torsional barriers for [3]ferrocenophane bridge bonds, numbers in parenthesis are values quoted in the literature (see text).

ber of other values of  $\Delta V$ . For example the difference between the C—O and C—S torsional barriers  $\Delta V(\text{C} - \text{X})$  may be calculated from the values of  $\Delta G^\ddagger$  for  $\text{Cp}_2\text{Fe}(\text{CH}_2)_2\text{X}$  ( $\text{X} = \text{O}$  or  $\text{S}$ ) i.e.  $\Delta V = (39.7 - 34.7)/2 = 2.5 \text{ kJ mol}^{-1}$ . This value compares favourably with a value for  $\Delta V(\text{C} - \text{X})$  of  $1.6 \text{ kJ mol}^{-1}$  calculated from Me—X torsional barriers in Me—X—Me ( $\text{X} = \text{O}$  or  $\text{S}$ ) [16]. Similarly comparing values of  $\Delta G^\ddagger$  for  $\text{Cp}_2\text{FeS}_2\text{S}$  [4] and  $\text{Cp}_2\text{FeS}_2\text{CH}_2$ , Table 4, gives a value of  $\Delta V(\text{X} - \text{S}; \text{X} = \text{S}$  or  $\text{C})$  of  $16.4 \text{ kJ mol}^{-1}$ . A variety of other relative torsional barriers may also be determined in this way and are illustrated in Fig. 7.

It should be noted that if we assume a value of  $29.0 \text{ kJ mol}^{-1}$  for the absolute S—S torsional barrier [4], our data predict an absolute torsional barrier about the C—S bond in [3]ferrocenophanes of  $29.0 - 16.4 = 12.6 \text{ kJ mol}^{-1}$  which compares to that of  $8.9 \text{ kJ mol}^{-1}$  determined directly by studies on Me—S—Me [16], the difference between these two values reflecting the different carbon atom environments. In a similar way other absolute torsional barriers in [3]ferrocenophanes have been calculated and are shown in Fig. 7. The figure also incorporates our previously published data [4] for chalcogen bonds.

#### *Barriers to bridge and ring reversal*

It is interesting to compare the bridge reversal barriers determined for [3]ferrocenophanes, Table 4, with those for ring reversal in the analogous six-membered rings. In order to obtain the most reliable comparisons, the  $\Delta G^\ddagger$  (298 K) values computed for the bridge reversal process were converted to  $\Delta G^\ddagger(T_c)$  values, where  $T_c$  is the coalescence temperature of the ring reversal process in the corresponding six-membered ring compound. In this way the values of  $\Delta\Delta G^\ddagger(T_c)$  quoted in Table 3 to represent the energy difference between these two conformational processes are least susceptible to experimental error [9].

The  $\Delta G^\ddagger(T_c)$  data shown in Table 3 exhibit similar trends for the two types of motion, e.g. the replacement of the central sulphur atom with a methylene, in either  $\text{Cp}_2\text{FeS}_2\text{S}$  or  $(\text{CH}_2)_3\text{S}_2\text{S}$ , brings about a reduction in energy barrier. Such similarities are clear indication that the two different fluxional motions proceed via analogous mechanisms [4] with the torsional energies of the relevant bridge bonds being the major contributors to the total energy barrier.

The values of  $\Delta\Delta G^\ddagger(T_c)$  listed in Table 3 appear to reflect a variable influence of the  $\text{Cp}_2\text{Fe}$  moiety on the energy barrier. For example in all cases where sulphur atoms are adjacent to the  $\text{Cp}_2\text{Fe}$  or  $(\text{CH}_2)_3$  moieties  $\Delta G^\ddagger$  (bridge reversal, B.R.)  $>$   $\Delta G^\ddagger$  (ring reversal, R.R.) whereas in compounds having methylene groups adjacent to  $\text{Cp}_2\text{Fe}$  or  $(\text{CH}_2)_3$ ,  $\Delta G^\ddagger$  (B.R.)  $<$   $\Delta G^\ddagger$  (R.R.). These trends must partially reflect different signs of  $\Delta V(\text{C} - \text{X})$  for the cases when the carbon atom is part of a  $\text{Cp}_2\text{Fe}$  moiety and when it is part of a  $(\text{CH}_2)_3$  moiety. In particular, when  $\text{X} = \text{S}$  then  $\Delta V$  is greater for the  $\text{Cp}_2\text{Fe}$  case and when  $\text{X} = \text{C}$ , it is greater for the  $(\text{CH}_2)_3$  moiety. However if this was the only explanation values of  $\Delta\Delta G^\ddagger(T_c)$  would be equal in the three cases where sulphur (or carbon) atoms are attached to the moieties in question, and this is clearly not the case.

Since the values of  $\Delta G^\ddagger(T_c)$  for bridge reversal are found to have a much wider energy range than those for ring reversal an alternative explanation is that

$\Delta G^\ddagger(T_c)$  is much more sensitive to the  $X_2Y$  bridge length for  $Cp_2FeX_2Y$  than for  $(CH_2)_3X_2Y$ .

### Acknowledgments

We are indebted to Dr. V. Šik for recording the NMR spectra, and to the S.R.C. for the use of facilities at the P.C.M.U. Harwell.

### References

- 1 E.W. Abel, M. Booth and K.G. Orrell, *J. Organometal. Chem.*, **160** (1978) 75.
- 2 E.W. Abel, M. Booth and K.G. Orrell, *J. Chem. Soc. Dalton*, (1980) 1582.
- 3 E.W. Abel, M. Booth and K.G. Orrell, *J. Organometal. Chem.*, **186** (1980) C37.
- 4 E.W. Abel, M. Booth and K.G. Orrell, *J. Organometal. Chem.*, **208** (1981) 213.
- 5 M. Rosenblum, A.K. Banerjee, N. Danieli, R.W. Fish and V. Schlatter, *J. Amer. Chem. Soc.*, **85** (1963) 316.
- 6 K. Yamakawa and M. Hisatome, *J. Organometal. Chem.*, **52** (1973) 407.
- 7 A. Davison and J.C. Smart, *J. Organometal. Chem.*, **174** (1979) 321.
- 8 G. Binsch in L.M. Jackman and F.A. Cotton (Eds.), *Dynamic Nuclear Magnetic Resonance Spectroscopy*, Academic Press, New York, 1975, p. 45.
- 9 G. Binsch and H. Kessler, *Angew. Chemie, Int. Edit.*, **19** (1980) 411.
- 10 T.H. Barr and W.E. Watts, *Tetrahedron*, **24** (1968) 6111.
- 11 R.R. McGuire, R.E. Cochoy and J.A. Winstead, *J. Organometal. Chem.*, **84** (1975) 269.
- 12 E.W. Abel, M. Booth and K.G. Orrell, *J. Chem. Soc. Dalton*, (1980) 1994.
- 13 I. Bernal and B.R. Davis, *J. Cryst. Mol. Struct.*, **2** (1972) 107.
- 14 A.G. Osborne, R.E. Hollands, J.A.K. Howard and R.F. Bryan, *J. Organometal. Chem.*, **205** (1981) 395.
- 15 G. Binsch, D. Höfner and S.A. Lesko, *Org. Magn. Reson.*, **11** (1978) 179.
- 16 J.B. Lambert and S.I. Featherman, *Chem. Revs.*, **75** (1975) 611.
- 17 H. Friebolin, S. Kabuss, A. Luttringhaus and R. Mecke, *Z. Naturforsch. B.* **21** (1966) 320.
- 18 W. Faisst, H. Friebolin, S. Kabuss and H.G. Schmid, *Org. Magn. Reson.*, **1** (1969) 67.
- 19 F.A.L. Anet and A.J.R. Bourn, *J. Amer. Chem. Soc.*, **99** (1967) 760.
- 20 D.H. Johnson, J.B. Lambert and C.E. Mixan, *J. Amer. Chem. Soc.*, **95** (1973) 4634.